Proceedings of IMECE2002
ASME International Mechanical Engineering Congress & Exposition
November 17-22, 2002, New Orleans, Louisiana
Paper Number: IMECE2002-MED-33723

# Investigation of Thermal Effect of Packaged CMOS Compatible Pressure Sensor

**Chih-Tang Peng[1], Ji-Cheng Lin[1], Chun-Te Lin[1], Kuo-Ning Chiang[2]**

E-Mail: Knchiang@pme.nthu.edu.tw

Department of Power Mechanical Engineering

National Tsing Hua University

Hsin Chu, Taiwan 300, R.O.C.

## Abstract

In this study, a packaged silicon base piezoresistive pressure sensor with thermal stress buffer is designed, fabricated, and measured. A finite element method (FEM) is adopted for design and experimental validation of the sensor performance. Thermal and pressure loading on the sensor is applied to make a comparison between sensor experimental and simulation results. Furthermore, a method that transfers simulation stress data into output voltage is proposed in this study, the results indicate that the experimental result coincides with simulation data.

Keywords: Piezoresistive pressure sensor, finite element method (FEM).

---

[1]. Graduate Assistant, Ph.D candidate

[2] . Corresponding Author, Associate Professor, Dept. of Power Mechanical Engineering, National Tsing Hua University

## Ⅰ. Introduction

Since piezoresistive effect is discovered, the applications of piezoresistive sensor are widely employed in mechanical signal sensing. Silicon base pressure sensor is one of the major applications of the piezoresistive sensor. Nowadays, silicon piezoresistive pressure sensor is a mature technology in industry and its measurement accuracy is more rigorous in many advanced applications. Therefore, the thermal and packaging effects should be taken into consideration for a better sensor accuracy.

The fundamental concept of piezoresistive effect is the change in resistive of a material causing from an applied stress. This effect in silicon material was first discovered by Smith [1], and Adams [2] in 1950's and was applied extensively in mechanical signal measurement for years. Smith proposed the change in conductivity under stress in bulk n-type material and designed an experiment to measure the longitudinal as well as transverse piezoresistance coefficients. Pfann [3] presented the shear piezoresistance effect, he designed several types of semiconductor stress gauge to measure the longitudinal, transverse, shear stress and torque, and a Wheastone bridge type gauge is employed in mechanical signal measurement. Piezoresistance coefficient is a function of impurity concentration and temperature; hence the thermal effect will influence the measurement result of a piezoresistive sensor. Kanda [4] produced a piezoresistance coefficient study about orientations, impurity concentration and temperature. Lund [5] also studied the temperature dependency of piezoresistance coefficient by four points bending experiment. Piezoresistive effect on polysilicon is another method to apply for mechanical signal sensing, French [6] presented the piezoresistive effect in polysilicon and its applications to strain gauges. In French's study, a comparison is made between theory and experiment for longitudinal and transverse strain measurement of n-type and p-type materials.

Piezoresistive pressure sensor design is widely studied at 1990's in MEMS and electronic packaging field. Kanda [7] applied MEMS process to fabricate piezoresistive pressure sensors on {100} and {110} wafer for optimum design considerations. Recently, finite element analysis (FEA) is widely adopted for stress prediction, thermal effect reduction, packaging design and reliability enhancement of piezoresistive sensor. Pancewicz [8] used FEA to obtain the output voltage of the pressure sensor and compared the simulation data with experiment result. Schilling [9] also applied FEA for sensor performance simulation and discussed the packaging effects on silicon piezoresistive pressure sensors. Jaeger [10], [11] employed piezoresistive sensor made on silicon chip to measure the stresses in electronic packaging devices.

In this research, a comparison between experiment and FEA is accomplished. In the case studies, the FEA demonstrated promising results for sensor performance prediction.

## Ⅱ. Theory

- Fundamental theory of piezoresistance:

The piezoresistive effect is the change in resistive of a material causing from an applied loading. In this section, the mathematical description of piezoresistance that influence of stresses is introduced. For a three-dimensional anisotropic crystal, the electric field vector (E) is related to the current vector (i) by a three-by-three resistivity tensor (ρ). Experimentally, the nine resistivity coefficients could be reduced to six and become a symmetrical matrix:

$$\begin{bmatrix} E_1 \\ E_2 \\ E_3 \end{bmatrix} = \begin{bmatrix} \rho_1 & \rho_6 & \rho_5 \\ \rho_6 & \rho_2 & \rho_4 \\ \rho_5 & \rho_4 & \rho_3 \end{bmatrix} \begin{bmatrix} i_1 \\ i_2 \\ i_3 \end{bmatrix} \tag{1}$$

The resistivity change in the isotropic silicon can be obtained as follow:

$$\begin{bmatrix} \rho_1 \\ \rho_2 \\ \rho_3 \\ \rho_4 \\ \rho_5 \\ \rho_6 \end{bmatrix} = \begin{bmatrix} \rho \\ \rho \\ \rho \\ 0 \\ 0 \\ 0 \end{bmatrix} + \begin{bmatrix} \Delta\rho_1 \\ \Delta\rho_2 \\ \Delta\rho_3 \\ \Delta\rho_4 \\ \Delta\rho_5 \\ \Delta\rho_6 \end{bmatrix} \tag{2}$$

Where $\Delta\rho$ is the resistivity change.

Based on the mechanics theory definition, the stresses are defined as six components: three normal stresses $\sigma_x$, $\sigma_y$, and $\sigma_z$, along the cubic crystal axis, and three shear stresses $\tau_{xy}$, $\tau_{yz}$, and $\tau_{xz}$. To obtain the relation between resistivity and stresses, piezoresistance coefficients $\pi_{ij}$ (expressed in $Pa^{-1}$) are defined as a six by six matrix. For the cubic crystal structure of silicon, due to the symmetry conditions, the coefficients of matrix can reduce to three independent components: $\pi_{11}$, $\pi_{12}$, and $\pi_{44}$. Equation (3) depicts the resistivity variations and the stress relation:

$$\frac{1}{\rho}\begin{bmatrix}\Delta\rho_1\\ \Delta\rho_2\\ \Delta\rho_3\\ \Delta\rho_4\\ \Delta\rho_5\\ \Delta\rho_6\end{bmatrix}=\begin{bmatrix}\pi_{11} & \pi_{12} & \pi_{12} & 0 & 0 & 0\\ \pi_{12} & \pi_{11} & \pi_{12} & 0 & 0 & 0\\ \pi_{12} & \pi_{12} & \pi_{11} & 0 & 0 & 0\\ 0 & 0 & 0 & \pi_{44} & 0 & 0\\ 0 & 0 & 0 & 0 & \pi_{44} & 0\\ 0 & 0 & 0 & 0 & 0 & \pi_{44}\end{bmatrix}\begin{bmatrix}\sigma_x\\ \sigma_y\\ \sigma_z\\ \tau_{yz}\\ \tau_{xz}\\ \tau_{xy}\end{bmatrix} \quad (3)$$

Combining equations 1,2, and 3, the electric field in a cubic crystal lattice under stress is obtained:

$$\begin{aligned}E_1 &= \rho i_1 + \rho\pi_{11}\sigma_x i_1 + \rho\pi_{12}(\sigma_y + \sigma_z)i_1 + \rho\pi_{44}(i_2\tau_{xy} + i_3\tau_{xz})\\ E_2 &= \rho i_2 + \rho\pi_{11}\sigma_y i_2 + \rho\pi_{12}(\sigma_x + \sigma_z)i_2 + \rho\pi_{44}(i_1\tau_{xy} + i_3\tau_{yz})\\ E_3 &= \rho i_3 + \rho\pi_{11}\sigma_z i_3 + \rho\pi_{12}(\sigma_x + \sigma_y)i_3 + \rho\pi_{44}(i_1\tau_{xz} + i_2\tau_{yz})\end{aligned} \quad (4)$$

In order to derive the stresses and the electric field expressed in an arbitrary Cartesian system, the <100> axis should be transformed into the given coordinate system. Consider two Cartesian coordinate systems x'y'z' and xyz, these two systems are related by the direction cosines. Table 1 shows the notation corresponding to a complete set of directional cosines.

Table 1. Complete set of directional cosines

| | x | y | z |
|---|---|---|---|
| x' | $l_1$=cos(x',x) | $m_1$=cos(x',y) | $n_1$=cos(x',z) |
| y' | $l_2$=cos(y',x) | $m_2$=cos(y',y) | $n_2$=cos(y',z) |
| z' | $l_3$=cos(z',x) | $m_3$=cos(z',y) | $n_3$=cos(z',z) |

Equation 5 indicates the vector (x, y, z) referred to the crystal axis transformed into a vector (x, y, z):

$$\begin{bmatrix}x'\\ y'\\ z'\end{bmatrix}=\begin{bmatrix}l_1 & m_1 & n_1\\ l_2 & m_2 & n_2\\ l_3 & m_3 & n_3\end{bmatrix}\begin{bmatrix}x\\ y\\ z\end{bmatrix} \quad (5)$$

The axis transformation of equation 5 is applied to equation 4:

$$E' = \rho i' + \rho i'\left[\pi_{11} + 2(\pi_{44} + \pi_{12} - \pi_{11})(l_1^2 m_1^2 + l_1^2 n_1^2 + m_1^2 n_1^2)\right] \quad (6)$$

From equation 6, the longitudinal and transverse piezoresistance coefficients can be defined as follow:

$$\pi_l = \pi_{11} + 2(\pi_{44} + \pi_{12} - \pi_{11})(l_1^2 m_1^2 + l_1^2 n_1^2 + m_1^2 n_1^2) \quad (7)$$

$$\pi_t = \pi_{12} - (\pi_{44} + \pi_{12} - \pi_{11})(l_1^2 l_2^2 + m_1^2 m_2^2 + n_1^2 n_2^2) \quad (8)$$

There is a contribution to resistance change from longitudinal ($\sigma_l$) and transverse ($\sigma_t$) stresses with respect to the current flow. The mechanical stresses and the total resistance change (ΔR) relation can be expressed as follow:

$$\frac{\Delta R}{R} = \sigma_l \pi_l + \sigma_t \pi_t \quad (9)$$

Where R is the zero-stress resistance and ΔR is the resistance change, respectively.

- Wheatstone bridge to piezoresistive sensor:

Figure 1 illustrates a membrane with four piezoresistors.

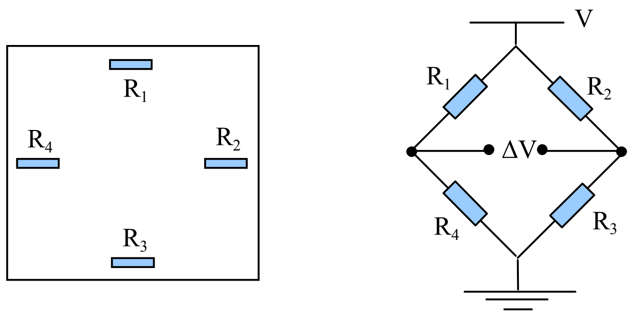


Fig. 1: Four piezoresistors on a membrane and Wheatstone bridge configuration of the four piezoresistors

Two resistors are oriented to sense stress in the direction of their current axis and two are placed to sense stress perpendicular to their current flow. If the resistors are correctly positioned on the membrane, the resistance change of the first two piezoresistors will be opposite to that of the other two. Thereby the absolute value of the four-resistance variation could be equal. The resistors are connected in a Wheatstone bridge (shows in Fig.1), where V is bridge-input voltage, ΔV is differential output voltage. The resistance change due to unbalanced bridge can directly convert into voltage signal under an applied pressure. Equation 10 shows the voltage and resistance relation:

$$\frac{\Delta V}{V} = \frac{\Delta R}{R} \quad (10)$$

Where ΔR is resistance changes, $R = |R_1| = |R_2| = |R_3| = |R_4|$ is the zero-stress resistance.

- The relationship of stresses and output voltage:

The mechanical stresses obtained by FEA should be transferred into output voltage thus the simulation stress value can be applied to predict the equivalent output electrical signal. Equation 11 indicates the output voltage, resistance and stresses variation relation:

$$\frac{\Delta V}{V} = \frac{\Delta R}{R} = \frac{\pi_l(\sum_{i=1}^{n} \sigma_{li} v_i) + \pi_t(\sum_{i=1}^{n} \sigma_{ti} v_i)}{\sum_{i=1}^{n} v_i} \tag{11}$$

Where ΔV is differential output voltage, V is bridge-input voltage, ΔR is resistance changes, R is the zero-stress resistance, $\pi_l$ and $\pi_t$ are the longitudinal and transverse piezoresistance coefficients, i is the piezoresistive element number of finite element model, $\sigma_{li}$ and $\sigma_{ti}$ are the longitudinal and transverse stresses of the $i^{th}$ piezoresistive element, $v_i$ is the volume of the $i^{th}$ element on the piezoresistors. Figure 2 illustrates a quarter of finite element model. By applying this transfer method, the FEA simulation can employ to predict the output signal of the piezoresistive pressure sensor.

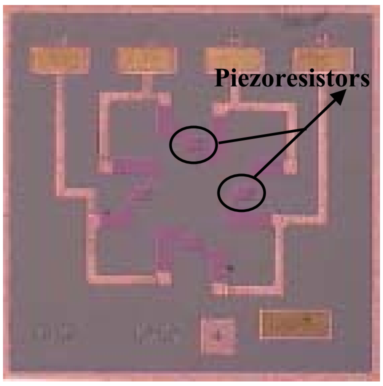


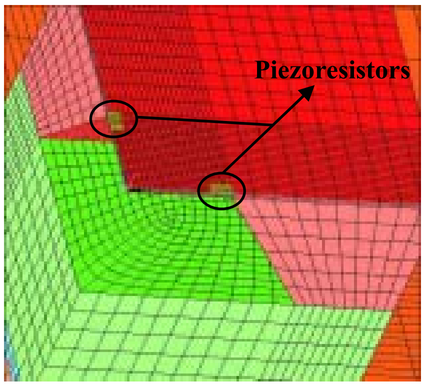


Fig. 2: Piezoresistors on the quarter of finite element model

## Ⅲ. Comparison of finite element analysis and experiment results

In order to demonstrate the feasibility of the finite element analysis on sensor design, a prototype silicon base piezoresistive pressure sensor is fabricated and several pressure with thermal loading are applied on the sensor.

- Fabrication and experiment:

A piezoresistive pressure sensor is fabricated in this study. Figure 3 indicates the sensor fabrication process.

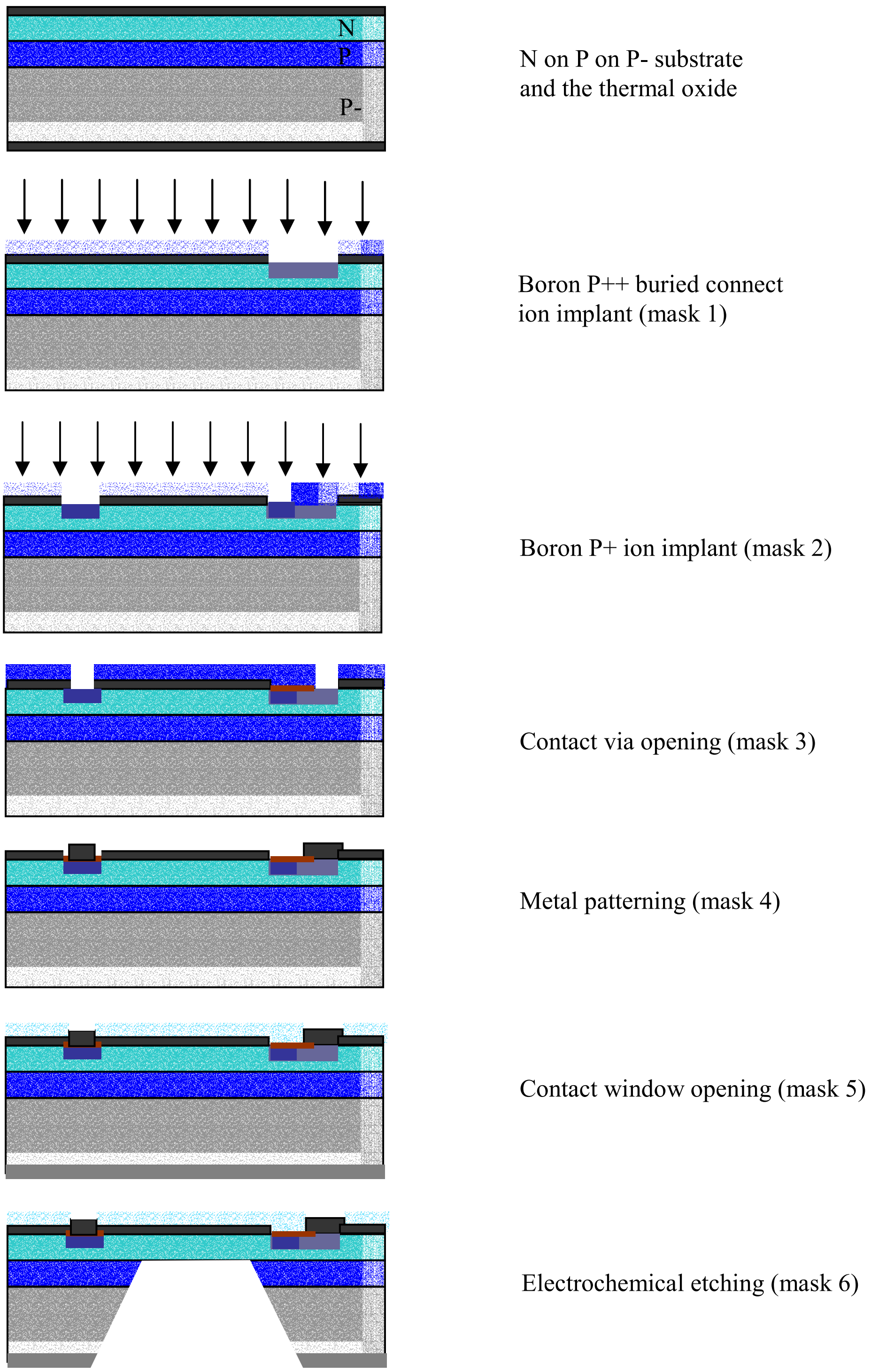

Fig. 3: Piezoresistive pressure sensor fabrication process

This sensor is fabricated by CMOS compatible process (except the anisotropic etching process) with six masks processing. A p-type silicon wafer with <100> plane is used as a substrate for sensor fabrication. The piezoresistors connected in a Wheatstone bridge are located at $(110)$ for longitudinal direction and $(1\bar{1}0)$ for transverse direction. Figure 4 illustrates the top view of the sensor.

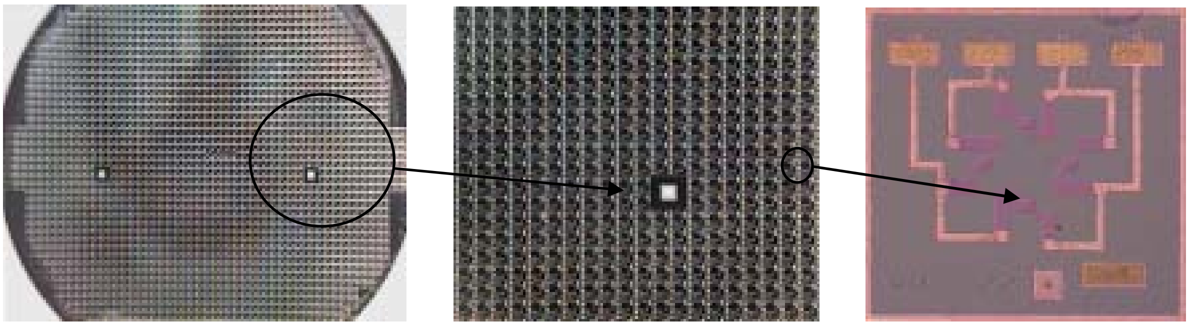

Fig. 4: Top view of a piezoresistive pressure sensor (bare die)

This pressure sensing device is composed by four parts: a PCB substrate, a glass substrate bonding with silicon, an adhesive layer between PCB and glass, and a membrane made by silicon with piezoresistive sensing units on it. Figure 5 illustrates the structure cross section and top view of this packaged pressure sensor. Table 2 indicates the dimensions of the fabricated sensor.

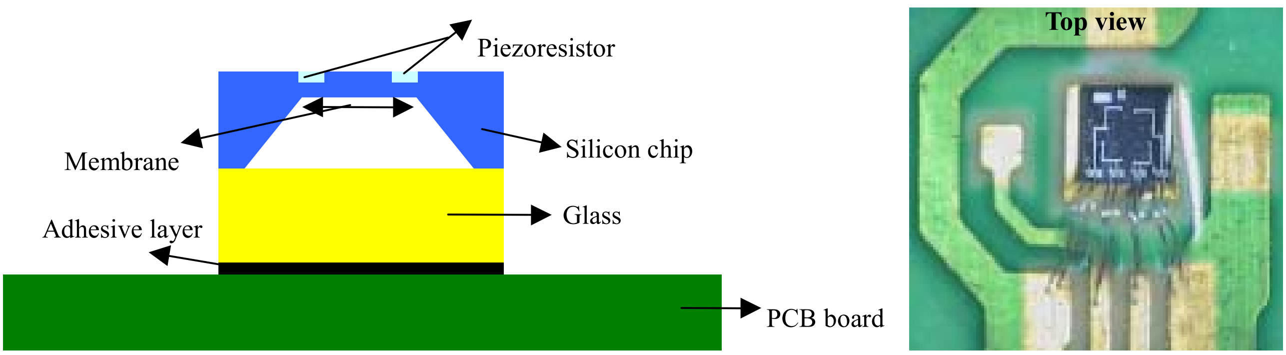


Fig. 5: The structure cross section and top view of the packaged pressure sensor

Table 2. Dimensions of PCB, glass, adhesive layer, silicon chip and silicon membrane

| Layer | Length (μm) | Width (μm) | Thickness (μm) |
|---|---|---|---|
| PCB | 10000 | 10000 | 1200 |
| Glass | 1800 | 1800 | 500 |
| Adhesive | 1800 | 1800 | 50 |
| Silicon Chip | 1800 | 1800 | 450 |
| Silicon Membrane | 600 | 600 | 20 |

The packaged pressure sensor are tested at 10psi and 20psi pressure loading with -10℃ to 60℃ environmental conditions, and the input voltage is 5V. Figure 8 to 11 present the measurement result.

- Finite element analysis:

In order to analyze the performance of the pressure sensor, the finite element analysis is employed to analyze mechanical signal change due to thermal and pressure loading. In this study, the ANSYS finite element program is used. A three-dimensional eight-nodes element is adopted in this analysis.

A finite element model is established as a quarter model in Fig. 6, since the packaged pressure sensor device possesses quartered symmetry.

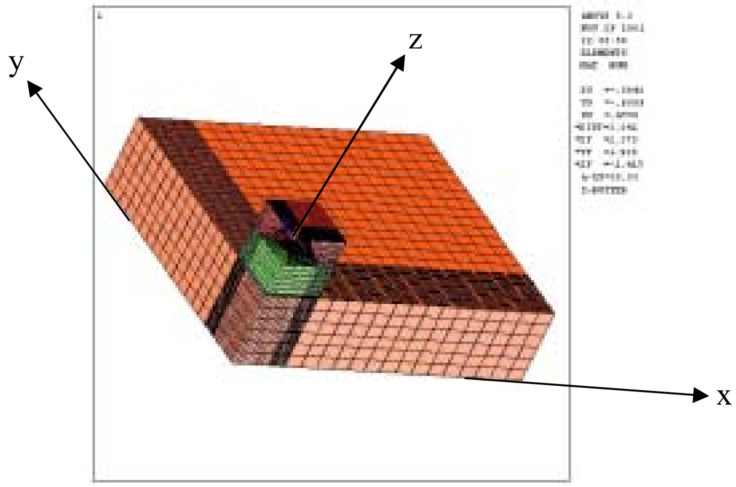


Fig. 6: One-quarter finite element model of piezoresistive pressure sensor

This finite element model contains 23,450 elements and 79,614 D.O.F. The boundary condition is with all nodes fixed in x, y, and z directions on the bottom side of PCB substrate and a symmetry condition is conducted on the xz and yz planes. The loading conditions are 10psi and 20psi pressure loading with the temperature of -10℃ to 60℃ environmental condition, and stress free temperature is 25℃.

Table 3 indicates the material properties of PCB (FR-4), glass (7740), adhesive layer, and silicon.

Table 3. Material properties of PCB (FR-4), glass (7740), adhesive, and silicon

| Layer | Young's Modulus (Gpa) | Poisson's Ratio | CTE (1/℃) |
|---|---|---|---|
| PCB (FR-4) | 18 | 0.19 | 16ppm |
| Glass (7740) | 76 | 0.28 | 3.25ppm |
| Adhesive | 8.96 | 0.25 | 15ppm |
| Silicon | 112.4 | 0.28 | 2.62ppm |

In this study, owing to the piezoresistive coefficient is a function of temperature, the temperature coefficient of piezoresistor should be taken into consideration. Figure 7 presents piezoresistance factor which influence by temperature and impurity concentration for p-type silicon, where piezoresistance $\pi(N, T) = \pi_0 * P(N, T)$, N is doping concentration, T is temperature, $\pi_0$ is piezoresistive coefficient at low-doped and room temperature condition and P(N, T) is piezoresistance factor. A semiconductor fabrication process simulation software "TSUPREM" is applied in this work to obtain the doping concentration value of the piezoresistor.

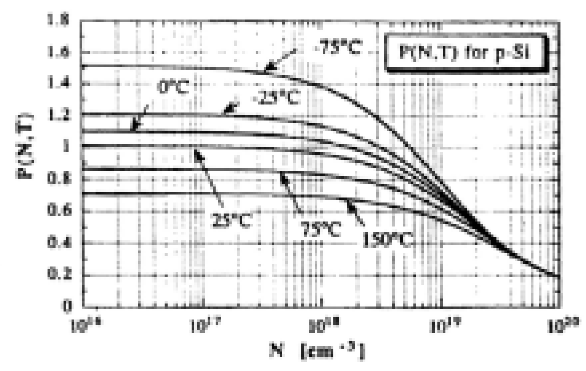


Fig. 7: Piezoresistance factor influenced by temperature and doping concentration (ref. [12])

It is obtained in "TSUPREM" calculation result that after annealing, the doping concentration value of the piezoresistor is $3.5*10^{18}$(cm$^{-3}$), hence the piezoresistance value that varies with temperature at this doping concentration can be applied in the simulation data.

The longitudinal and transverse piezoresistance coefficients of this sensor are $\pi_l = 1/2(\pi_{11}+\pi_{12}+\pi_{44})$ and $\pi_t = 1/2(\pi_{11}+\pi_{12}-\pi_{44})$, where $\pi_{11} = 6.6*10^{-11}$ ($Pa^{-1}$), $\pi_{12} = -1.1*10^{-11}$ ($Pa^{-1}$), and $\pi_{44} = 138.1*10^{-11}$ ($Pa^{-1}$) (p-type silicon at low doped value and room temperature condition, ref. [1]), respectively. The calculated longitudinal as well as transverse stresses are used to calculate the differential output voltage.

Figure 8 to 11 present the FEA simulation and experimental value results. It is observed that the FEA gave a promising result with the experimental data, the average error between FEA and experiment is less than 3.5 %, thereby demonstrating that FEA can predict the mechanics signal output of the pressure sensor accurately. Based on the above validation, the FEA method can be applied to study sensor performance, thermal and packaging effects in the pressure sensor research.

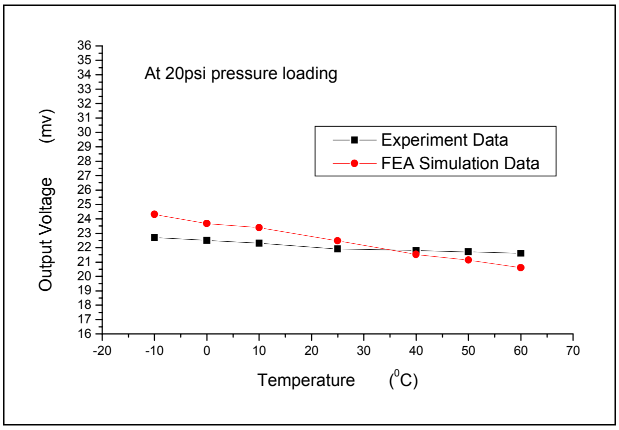


Fig. 8: FEA simulation and experiment data comparison result (at 10psi)

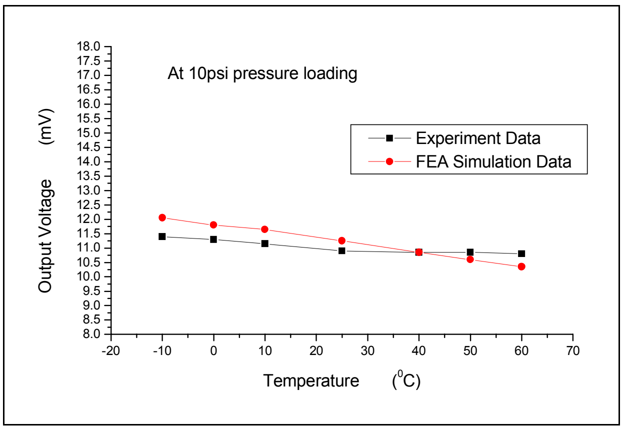


Fig. 9: FEA simulation and experiment data comparison result (at 20psi)

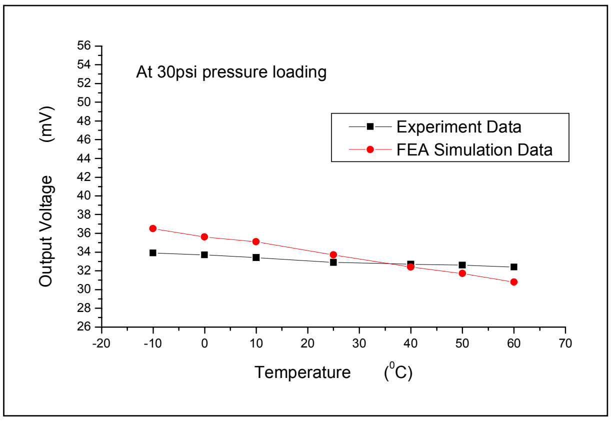


Fig. 10: FEA simulation and experiment data comparison result (at 30psi)

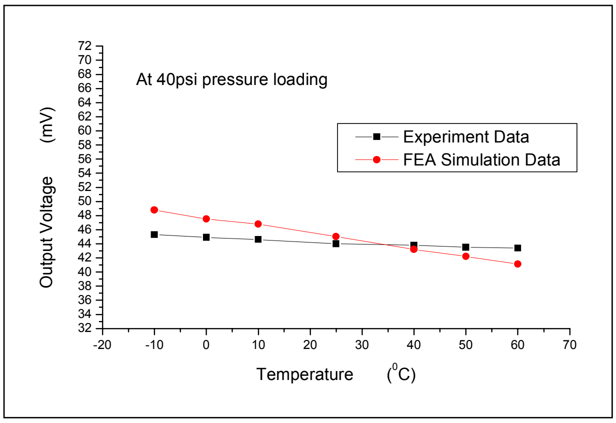


Fig. 11: FEA simulation and experiment data comparison result (at 40psi)

## Ⅳ. Conclusions

In accordance with the well correlation between experimental and FEA results. The following conclusions are addressed: The method proposed in this work for transferring the mechanical stresses of FEA data into output voltage is feasible, thus confirming that FEA can predict the external pressure loading behavior of the pressure sensor accurately, and it is a reliable tool for the sensor performance design.

## References

[1] C.S. Smith, 1954, "Piezoresistance Effect in Germanium and Silicon," Physical Review,

Vol.94, pp.42-49.

[2] E.N. Adams, 1954, “Phys.,” Vol.96, pp.803.

[3] W.G. Pfann and R.N. Thurston, 1961, “Semiconducting Stress Transducers Utilizing the Transverse and Shear Piezoresistance Effects,” Journal of Applied Physics, Vol.32, pp. 2008-2018.

[4] Y. Kanda, 1982, “A Graphical Representation of the Piezoresistance Coefficient in Silicon,” IEEE Transactions on Electron Devices, Vol. ED-29, No.1, pp.64-70.

[5] E. lund and T. Finstad, 1999, “Measurement of the Temperature Dependency of the Piezoresistance Coefficients in P-Type Silicon,” Advances in Electronic Packaging-ASME, EEP-Vol. 26-1, pp.215-218.

[6] P.J. French and A.G.R. Evans, 1989, “Piezoresistance in Polysilicon and Its Applications to Strain Gauges,” Solid-State Electronics, Vol.32, No.1, pp.1-10.

[7] Y. Kanda, 1997, “Optimum Design Considerations for Silicon Piezoresistive Pressure Sensor,” Sensor and Actuators, A62, pp.539-542.

[8] T. Pancewicz, R. Jachowicz, Z. Gniazdowski, Z. Azgin, P. Kowalski, 1999, “The Empirical Verification of the FEM Model of Semiconductor Pressure Sensor,” Sensor and Actuators, 76, pp.260-265.

[9] F. Schilling, W. Langheinrich, K. Weiblen and D. Arand, 1997, ”Simulation of Thermally Induced Package Effects with Regard to Piezoresistive Pressure Sensors,” Sensor and Actuators, A60, pp.37-39.

[10] R.C Jaeger, J.C Suhling, M.T Carey, and R.W Johnson, 1993, “A Piezoresistive Sensor Chip for Measurement of Stress in Electronic Packaging,” IEEE, pp.686-692.

[11] R.C Jaeger, J.C Suhling, A.T Bradley, and J.Xu, 1999, “Silicon Piezoresistive Stress Sensors Using MOS and Bipolar Transistors,” Advances in Electronic Packaging-ASME, EEP-Vol. 26-1, pp.219-225.

[12] S.M. Sze, 1994, “Semiconductor Sensors,” pp.173, John Wiley & Sons.